

Pyrrolo[3,2,1-kl]phenothiazine-based D- π -A type organic dyes for efficient dye-sensitized solar cells



Feng Li ^{a,b}, Yi-Zhou Zhu ^{a,**}, Shao-Chun Zhang ^a, Huan-Huan Gao ^a, Bin Pan ^a, Jian-Yu Zheng ^{a,b,*}

^a State Key Laboratory and Institute of Elemento-Organic Chemistry, Nankai University, Tianjin 300071, China

^b Collaborative Innovation Center of Chemical Science and Engineering (Tianjin), Nankai University, Tianjin 300071, China

ARTICLE INFO

Article history:

Received 22 September 2016

Received in revised form

2 December 2016

Accepted 11 December 2016

Available online 18 December 2016

Keywords:

Dye-sensitized solar cells

Organic dyes

Pyrrolo[3,2,1-kl]phenothiazine

Conjugated linker

ABSTRACT

Novel metal-free organic dyes based on polycyclic aromatic donor, pyrrolo[3,2,1-kl]phenothiazine, have been synthesized and applied in dye-sensitized solar cells. Combined with cyanoacrylic acid as the acceptor/anchoring group and simple π -spacers such as thiophene (**JY40**), furan (**JY41**), and terthiophene (**JY42**) as the conjugated linker, these dyes show good power conversion efficiency (PCE). The photophysical, electrochemical and photovoltaic properties, as well as theoretical calculations of these dyes were fully investigated. An attractive PCE up to 7.54%, with a short-circuit photocurrent density (J_{SC}) of 17.76 mA cm⁻², an open-circuit photovoltage (V_{OC}) of 726 mV, and a fill factor (FF) of 0.58 has been achieved by the **JY42**-based cell under standard AM 1.5 G irradiation in conjunction with an iodine electrolyte.

© 2016 Published by Elsevier Ltd.

1. Introduction

As a promising photovoltaic technology, dye-sensitized solar cells (DSSCs) have attracted considerable attention during the past two decades because of their low cost, easy fabrication and impressive device efficiency [1,2]. Owing to the decisive influence of dyes on the device performance [3], various types of sensitizers including metal complexes, porphyrins and metal-free organic dyes have been successfully developed and applied in the highly efficient DSSCs. Although ruthenium(II) complexes have been early designed, and some well-known species such as **N3**, **N719** and black dye have achieved high conversion efficiency over 10% [4–6], high cost and potential negative environmental impact unavoidably limit their practical application in DSSCs. Research interests now concern more about the porphyrin-based dye [7–9] and metal-free organic dyes [10–12] due to the structural diversity, understandable design and facile modification. Recently, DSSC device sensitized by zinc-porphyrin **SM315** has reached an efficiency of ~13% by

using the Co^{II}/Co^{III} electrolyte under standard conditions [13]. Several high PCEs over 12% have also been achieved based on metal-free organic dyes [14–17]. However, how to get high device efficiency with a simple organic dye structure is still a challenge for DSSCs and calls for more efforts on it.

Generally, organic dyes are designed with donor- π -acceptor (D- π -A) configuration, for its intrinsic benefit in facilitating the intramolecular charge transfer (ICT) from the donor to the acceptor upon photoirradiation and subsequent electron injection into TiO₂ semiconductor anode. Structural variation of the donor, π -linker or acceptor will evidently tune the absorption spectra, orbital energy level and hence the photovoltaic performance of the resultant dye. Efforts upon novel donor, π -bridge, acceptor and their combination have been extensively made aiming at the improvement of DSSC performance. Besides the classic arylamine donor system [11,18–21], polycyclic aromatic ring has been reported to be attractive as a donor component.

Some devices with promising photovoltaic performance have been successfully fabricated using organic sensitizers containing polycyclic aromatic ring such as carbazole [15,22–24], phenothiazine [25–27], phenoxazine [28,29], *N*-annulated perylene [16,17,30] and indole derivatives [31,32] as the electron donors. To pursue greater photovoltaic device performance, new donors derived from abovementioned backbones with fusing heterocycles [33–36] or benzene rings [37] have been further synthesized and given

* Corresponding author. State Key Laboratory and Institute of Elemento-Organic Chemistry, Nankai University, Tianjin 300071, China.

** Corresponding author.

E-mail addresses: zhuyizhou@nankai.edu.cn (Y.-Z. Zhu), jyzheng@nankai.edu.cn (J.-Y. Zheng).

enhanced PCE. Pyrrolo[3,2,1-kl]phenothiazine [38,39], a fused tetracyclic system of phenothiazine, can be regarded to have both indole and phenothiazine components in core, which might show strong electron delocalization and significant potential for intramolecular charge transfer (ICT). As far as we are concerned, the photovoltaic application of pyrrolo[3,2,1-kl]phenothiazine derivatives has not been reported yet. Herein, novel organic sensitizers with pyrrolo[3,2,1-kl]phenothiazine as the electron donor and cyanoacrylic acid as the electron acceptor/anchoring group were designed and synthesized. For the purpose of gaining further insight into such system, different conjugated linkers such as thiophene (**JY40**), furan (**JY41**), and terthiophene (**JY42**) were chosen to act as the π -bridges. The chemical structures of these dyes are displayed in Fig. 1.

2. Experimental section

2.1. Materials and instruments

All solvents were purified according to standard methods. NMR solvents and other chemicals obtained from commercial sources were used without further purification. ^1H NMR and ^{13}C NMR spectra were recorded on Bruker 400 MHz spectrometer using TMS as the internal standard. HR-MS data were obtained on a VG ZAB-HS or Varian 7.0T FTMS. IR spectra were recorded with KBr pellets on a Bio-rad FTS6000 spectrometer. UV-vis spectra were recorded on a Varian Cary 300 Conc UV-visible spectrophotometer. Cyclic voltammetry and electrochemical impedance spectroscopy (EIS) experiments were carried out on a Zennium electrochemical workstation (Zahner Corporation).

2.2. Fabrication and characterization of DSSCs

The photoanode used was the TiO_2 thin film (~10 μm of 20 nm particles as the absorbing layer and ~4 μm of 200 nm particles as the scattering layer) coated on fluorine-doped tin oxide (FTO, Nippon Sheet Glass, $15\Omega/\text{sq}$) glass substrate by doctor-blade method. The resulting TiO_2 electrodes were gradually heated to 500 °C and sintered for 60 min, followed by treatment with TiCl_4 (0.04 M) aqueous solution at 70 °C for 60 min and sintered again at 500 °C for 60 min. The counter electrode was obtained by thermopyrolysis of H_2PtCl_6 (0.02 M in isopropanol) on the surface of FTO glass at 400 °C for 20 min. The adsorption of the dyes on TiO_2 was carried out in 0.3 mM dye solution in THF for 12 h. The electrolyte was composed of 0.3 M DMPII, 0.1 M LiI , 0.05 M I_2 and 0.5 M

4-*tert*-butylpyridine in acetonitrile. The DSSCs were illuminated by a solar simulator (CHF-XM-500W, Trusttech Co. Ltd.) under 100 mW cm^{-2} irradiation, which was calibrated by a standard silicon solar cell (91150 V, Newport Corporation). The photocurrent density-voltage (*J-V*) characteristic curves of the DSSC under simulated sunlight were recorded using an electrochemical workstation (Zahner Corporation). The incident photon-to-current conversion efficiency (IPCE) was measured using a commercial setup (QTest Station 2000 IPCE Measurement System, CROWN-TECH, USA).

2.3. Synthesis and characterization

2.3.1. 4-Bromo-2,6-diiodoaniline (**2**)

To a solution of 4-bromoaniline (6.88 g, 40 mmol) in anhydrous ethanol (200 mL), I_2 (22.34 g, 88 mmol) and Ag_2SO_4 (14.96 g, 48 mmol) were added. After stirring for 24 h at room temperature, the reaction mixture was filtered to remove AgI precipitate. The filtrate was concentrated under reduced pressure and dissolved in ethyl acetate. The organic layer was washed with aqueous $\text{Na}_2\text{S}_2\text{O}_3$ and brine, dried over Na_2SO_4 , filtered and concentrated. The crude product was purified by column chromatography on silica gel using CH_2Cl_2 /petroleum ether (1:6) as the eluent to afford compound **2** as a white solid (8.46 g, yield: 50%). ^1H NMR (400 MHz, CDCl_3) δ 7.73 (s, 2H), 4.63 (s, 2H). ^{13}C NMR (101 MHz, CDCl_3) δ 145.62, 140.97, 109.87, 81.03. IR (KBr) ν : 3399, 3300, 3195, 3061, 1731, 1607, 1548, 1439, 1341, 1280, 1232, 1107, 1053, 859, 701 cm^{-1} . HRMS (ESI): m/z [M+H] $^+$ calcd for $\text{C}_6\text{H}_5\text{BrI}_2\text{N}$, 423.7695; found, 423.7675.

2.3.2. 4-Bromo-2-((4-(hexyloxy)phenyl)ethynyl)-6-iodoaniline (**3**)

A mixture of compound **2** (3.55 g, 8.38 mmol), 1-ethyl-4-(hexyloxy)benzene (1.69 g, 8.35 mmol), $\text{Pd}(\text{PPh}_3)_2\text{Cl}_2$ (295 mg, 0.42 mmol) and CuI (161 mg, 0.84 mmol) in THF (20 mL) and triethylamine (20 mL) was stirred at room temperature for 18 h under a nitrogen atmosphere. The reaction mixture was filtered, and the filtrate was concentrated under reduced pressure. The crude product was purified by column chromatography on silica gel using CH_2Cl_2 /petroleum ether (1:3) as the eluent to afford compound **3** as a yellow solid (2.58 g, yield: 62%). ^1H NMR (400 MHz, CDCl_3) δ 7.69 (d, J = 2.2 Hz, 1H), 7.49–7.37 (m, 3H), 6.94–6.80 (m, 2H), 4.73 (s, 2H), 3.97 (t, J = 6.6 Hz, 2H), 1.78 (m, 2H), 1.52–1.40 (m, 2H), 1.40–1.28 (m, 4H), 0.91 (t, J = 7.0 Hz, 3H). ^{13}C NMR (101 MHz, CDCl_3) δ 159.84, 146.93, 140.51, 134.27, 133.21, 114.81, 114.20, 109.61, 108.92, 96.49, 83.07, 82.83, 68.29, 31.70, 29.27, 25.83, 22.74, 14.18. IR (KBr) ν : 3424, 3324, 2933, 2864, 2535, 2208, 1881, 1754, 1606, 1572, 1510, 1448, 1291, 1254, 1176, 1057, 1025, 855, 828, 725 cm^{-1} . HRMS (ESI): m/z [M+H] $^+$ calcd for $\text{C}_{20}\text{H}_{22}\text{BrINO}$, 497.9929; found, 497.9918.

2.3.3. 4-Bromo-1-(4-(hexyloxy)phenyl)pyrrolo[3,2,1-kl]phenothiazine (**4**)

In a 50 mL Schlenk tube, compound **3** (2.04 g, 4.1 mmol), CuI (79 mg, 0.41 mmol), dimethylglycine (85 mg, 0.82 mmol) and K_3PO_4 (2.18 g, 10.3 mmol) were added. The tube was evacuated and backfilled with nitrogen (three times). Then a solution of 2-bromobenzenethiol (1.18 g, 6.2 mmol) in DMSO (12.5 mL) was added via syringe. The mixture was stirred at 90 °C for about 18 h. Then it was stirred at 130 °C for 24 h. After being cooled to room temperature, the mixture was poured into water and extracted with ethyl acetate. The organic phase was washed with water for three times and dried over anhydrous Na_2SO_4 . After removal of the solvent under vacuum, the crude product was purified by column chromatography on silica gel using CH_2Cl_2 /petroleum ether (1:6) as the eluent to afford compound **4** as a white solid (870 mg, yield: 44%). ^1H NMR (400 MHz, CDCl_3) δ 7.45 (d, J = 8.7 Hz, 2H), 7.31 (d,

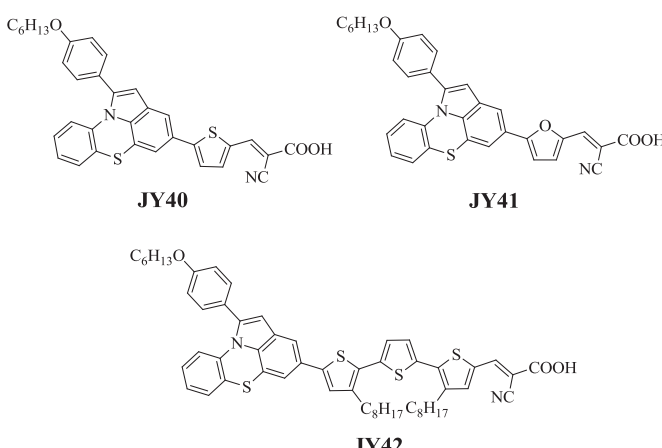


Fig. 1. Chemical structures of **JY40–42**.

$J = 1.3$ Hz, 1H), 7.13 (dd, $J = 7.7, 1.1$ Hz, 1H), 6.96 (d, $J = 8.7$ Hz, 2H), 6.93–6.87 (m, 2H), 6.86–6.78 (m, 1H), 6.72 (dd, $J = 8.3, 0.9$ Hz, 1H), 6.46 (s, 1H), 4.01 (t, $J = 6.5$ Hz, 2H), 1.96–1.71 (m, 2H), 1.55–1.44 (m, 2H), 1.37 (m, 4H), 0.93 (t, $J = 6.9$ Hz, 3H). ^{13}C NMR (101 MHz, CDCl_3) δ 159.68, 141.35, 136.42, 135.98, 129.81, 128.61, 128.21, 127.25, 125.45, 124.67, 122.35, 120.02, 119.80, 119.51, 119.35, 116.72, 114.98, 107.74, 68.32, 31.75, 29.38, 25.90, 22.76, 14.19. IR (KBr) ν : 3063, 2932, 2861, 2741, 1891, 1605, 1562, 1492, 1434, 1328, 1248, 1133, 1047, 1001, 935, 832, 790, 720 cm^{-1} . HRMS (ESI): m/z [M+H]⁺ calcd for $\text{C}_{26}\text{H}_{25}\text{BrNOS}$, 478.0840; found, 478.0832.

2.3.4. 5-(1-(4-(Hexyloxy)phenyl)pyrrolo[3,2,1-kl]phenothiazin-4-yl)thiophene-2-carbaldehyde (**6**)

A mixture of compound **4** (250 mg, 0.52 mmol), (5-formylthiophen-2-yl) boronic acid (162 mg, 1.04 mmol), Pd(dppf) $\text{Cl}_2\cdot\text{CH}_2\text{Cl}_2$ (45 mg, 0.055 mmol), K_2CO_3 (145 mg, 1.05 mmol) in toluene (10 mL) and methanol (2 mL) was stirred and heated at reflux for 5 h under a nitrogen atmosphere. After removal of the solvent, the crude product was purified by column chromatography on silica gel using $\text{CH}_2\text{Cl}_2/\text{petroleum ether}$ (1:1) as the eluent to afford compound **6** as a yellow solid (234 mg, yield: 88%). ^1H NMR (400 MHz, CDCl_3) δ 9.86 (s, 1H), 7.71 (d, $J = 3.9$ Hz, 1H), 7.49 (dd, $J = 13.2, 5.0$ Hz, 3H), 7.34 (d, $J = 3.9$ Hz, 1H), 7.17 (dd, $J = 7.7, 1.3$ Hz, 1H), 7.10 (d, $J = 1.4$ Hz, 1H), 7.01–6.94 (m, 2H), 6.94–6.89 (m, 1H), 6.88–6.80 (m, 1H), 6.75 (d, $J = 7.6$ Hz, 1H), 6.58 (s, 1H), 4.02 (t, $J = 6.5$ Hz, 2H), 1.89–1.75 (m, 2H), 1.49 (m, 2H), 1.38 (m, 4H), 0.93 (t, $J = 7.0$ Hz, 3H). ^{13}C NMR (101 MHz, CDCl_3) δ 182.83, 159.68, 155.37, 141.77, 141.63, 138.11, 137.72, 135.86, 129.80, 129.48, 128.24, 127.60, 127.25, 125.42, 124.81, 123.60, 122.42, 119.37, 115.90, 115.48, 114.97, 108.64, 68.31, 31.75, 29.37, 25.90, 22.76, 14.21. IR (KBr) ν : 3109, 3066, 2927, 2857, 2755, 1902, 1796, 1728, 1661, 1543, 1499, 1475, 1435, 1329, 1289, 1245, 1113, 1036, 900, 867, 807, 756 cm^{-1} . HRMS (MALDI-TOF): m/z [M+H]⁺ calcd for $\text{C}_{31}\text{H}_{28}\text{NO}_2\text{S}_2$, 510.1561; found, 510.1559.

2.3.5. 5-(1-(4-(Hexyloxy)phenyl)pyrrolo[3,2,1-kl]phenothiazin-4-yl)furan-2-carbaldehyde (**7**)

Compound **7** was synthesized by the same procedure described for **6** (yellow oil, 205 mg, yield: 81%). ^1H NMR (400 MHz, CD_2Cl_2) δ 9.58 (s, 1H), 7.69 (s, 1H), 7.47 (d, $J = 8.3$ Hz, 2H), 7.32 (d, $J = 3.6$ Hz, 1H), 7.26 (s, 1H), 7.18 (d, $J = 7.7$ Hz, 1H), 6.97 (d, $J = 8.3$ Hz, 2H), 6.93 (d, $J = 7.6$ Hz, 1H), 6.85 (t, $J = 7.8$ Hz, 1H), 6.80 (d, $J = 3.6$ Hz, 1H), 6.75 (d, $J = 8.3$ Hz, 1H), 6.61 (s, 1H), 4.02 (t, $J = 6.5$ Hz, 2H), 1.86–1.75 (m, 2H), 1.54–1.44 (m, 2H), 1.40–1.33 (m, 4H), 0.92 (t, $J = 6.4$ Hz, 3H). ^{13}C NMR (101 MHz, CDCl_3) δ 176.95, 160.27, 159.63, 151.73, 141.50, 138.15, 135.79, 129.77, 129.07, 128.19, 127.37, 127.16, 125.40, 125.25, 124.78, 122.49, 119.37, 119.19, 115.08, 114.93, 114.28, 108.73, 106.93, 68.28, 31.73, 29.35, 25.88, 22.74, 14.19. IR (KBr) ν : 3111, 3061, 2927, 2860, 2721, 1895, 1727, 1669, 1609, 1517, 1455, 1345, 1285, 1247, 1176, 1028, 969, 936, 838, 792, 756 cm^{-1} . HRMS (MALDI-TOF): m/z [M+H]⁺ calcd for $\text{C}_{31}\text{H}_{28}\text{NO}_3\text{S}$, 494.1790; found, 494.1789.

2.3.6. 5"--(1-(4-(Hexyloxy)phenyl)pyrrolo[3,2,1-kl]phenothiazin-4-yl)-3,3"-dioctyl-[2,2':5',2"-terthiophene]-5-carbaldehyde (**8**)

To a solution of compound **4** (215 mg, 0.45 mmol) in THF (10 mL), n-BuLi (0.37 mL, 0.59 mmol) was added drop-wise at -78°C under argon. The solution was stirred at the same temperature for 1 h, and $\text{B}(\text{OCH}_3)_3$ (85 mg, 0.81 mmol) was added. After stirring at the temperature for 4 h, the mixture was gradually warmed to room temperature and poured into water. Then CH_2Cl_2 was added, the organic phase was washed with water for three times and dried over anhydrous Na_2SO_4 . After removal of the solvent, the crude product was used for the next Suzuki reaction without purification. To a 100 mL Schlenk tube, the previous obtained crude product, compound **5** (105 mg, 0.18 mmol), Pd(dppf)

$\text{Cl}_2\cdot\text{CH}_2\text{Cl}_2$ (15 mg, 0.018 mmol), K_2CO_3 (150 mg, 1.08 mmol), toluene (10 mL) and methanol (2.5 mL) were added. The mixture was stirred at 90°C for 8 h under a nitrogen atmosphere. After removal of the solvent, the crude product was purified by column chromatography on silica gel using $\text{CH}_2\text{Cl}_2/\text{petroleum ether}$ (1:1) as the eluent to afford compound **8** as a red liquid (140 mg, yield: 87%). ^1H NMR (400 MHz, CDCl_3) δ 9.81 (s, 1H), 7.57 (s, 1H), 7.47 (d, $J = 8.6$ Hz, 2H), 7.40 (d, $J = 1.1$ Hz, 1H), 7.24 (d, $J = 3.8$ Hz, 1H), 7.16 (dd, $J = 7.6, 1.2$ Hz, 1H), 7.11 (d, $J = 3.9$ Hz, 2H), 7.06 (d, $J = 1.1$ Hz, 1H), 6.96 (d, $J = 8.7$ Hz, 2H), 6.91 (td, $J = 7.6, 1.1$ Hz, 1H), 6.85–6.79 (m, 1H), 6.76–6.71 (m, 1H), 6.53 (s, 1H), 4.01 (t, $J = 6.5$ Hz, 2H), 2.85–2.74 (m, 4H), 1.82 (m, 2H), 1.68 (dd, $J = 13.7, 6.5$ Hz, 4H), 1.54–1.47 (m, 2H), 1.46–1.28 (m, 24H), 0.94–0.87 (m, 9H). ^{13}C NMR (101 MHz, CDCl_3) δ 182.63, 159.54, 143.32, 141.41, 141.29, 141.20, 140.26, 140.11, 139.24, 138.82, 137.26, 136.10, 134.20, 130.34, 129.75, 128.61, 128.17, 127.95, 127.65, 127.09, 125.86, 125.78, 125.66, 124.54, 122.57, 119.25, 118.77, 115.14, 114.90, 114.65, 108.64, 68.28, 32.05, 32.01, 31.75, 30.73, 30.43, 29.91, 29.83, 29.67, 29.63, 29.57, 29.45, 29.40, 29.38, 25.90, 22.83, 22.82, 22.76, 14.27, 14.20. IR (KBr) ν : 3064, 2924, 2856, 2584, 1896, 1822, 1718, 1662, 1551, 1456, 1334, 1286, 1247, 1172, 1155, 1020, 936, 834, 796, 749 cm^{-1} . HRMS (MALDI-TOF): m/z [M+H]⁺ calcd for $\text{C}_{55}\text{H}_{64}\text{NO}_2\text{S}_4$, 898.3820; found, 898.3818.

2.3.7. (E)-2-Cyano-3-(5-(1-(4-(hexyloxy)phenyl)pyrrolo[3,2,1-kl]phenothiazin-4-yl)thiophen-2-yl)acrylic acid (**JY40**)

A mixture of compound **6** (222 mg, 0.44 mmol), cyanoacetic acid (186 mg, 2.19 mmol), ammonium acetate (255 mg, 3.3 mmol), and acetic acid (10 mL) was heated to reflux for 4 h under a nitrogen atmosphere. After cooling, it was poured into water and extracted with CH_2Cl_2 . The organic phase was washed with water for three times and dried over anhydrous Na_2SO_4 . The solvent was removed under vacuum, and the crude product was purified by column chromatography on silica gel using $\text{CH}_2\text{Cl}_2/\text{CH}_3\text{OH}$ (8:1) as the eluent to afford **JY40** as an orange solid (226 mg, yield: 89%). ^1H NMR (400 MHz, DMSO-d_6) δ 8.18 (s, 1H), 7.71 (d, $J = 3.8$ Hz, 1H), 7.56 (s, 2H), 7.44 (d, $J = 7.6$ Hz, 2H), 7.25 (d, $J = 4.4$ Hz, 2H), 6.99 (t, $J = 8.4$ Hz, 3H), 6.91 (t, $J = 7.7$ Hz, 1H), 6.74–6.61 (m, 2H), 4.00 (t, $J = 6.2$ Hz, 2H), 1.73 (m, 2H), 1.44 (m, 2H), 1.32 (d, $J = 3.5$ Hz, 4H), 0.89 (t, $J = 6.8$ Hz, 3H). ^{13}C NMR (101 MHz, DMSO-d_6) δ 164.06, 159.03, 149.83, 141.70, 140.87, 136.81, 135.15, 135.01, 129.38, 129.25, 128.16, 127.23, 124.88, 124.53, 123.93, 121.43, 118.61, 118.43, 115.12, 114.78, 108.60, 67.54, 31.02, 28.63, 25.20, 22.07, 13.87. IR (KBr) ν : 3034, 2931, 2862, 2215, 1892, 1602, 1501, 1467, 1393, 1289, 1247, 1179, 1063, 1019, 939, 839, 805, 753 cm^{-1} . HRMS (MALDI-TOF): m/z [M+H]⁺ calcd for $\text{C}_{34}\text{H}_{29}\text{N}_2\text{O}_3\text{S}_2$, 577.1620; found, 577.1620.

2.3.8. (E)-2-Cyano-3-(5-(1-(4-(hexyloxy)phenyl)pyrrolo[3,2,1-kl]phenothiazin-4-yl)furan-2-yl)acrylic acid (**JY41**)

JY41 was synthesized by the same procedure described for **JY40**, and the crude product was purified by column chromatography on silica gel using $\text{CH}_2\text{Cl}_2/\text{CH}_3\text{OH}$ (12:1) as the eluent to afford **JY41** as an orange solid (122 mg, yield: 84%). ^1H NMR (400 MHz, DMSO-d_6) δ 7.82 (s, 1H), 7.79 (s, 1H), 7.50 (d, $J = 8.6$ Hz, 2H), 7.46 (s, 1H), 7.32 (d, $J = 6.4$ Hz, 1H), 7.26 (s, 1H), 7.20 (d, $J = 3.5$ Hz, 1H), 7.03 (m, 3H), 6.96 (t, $J = 7.8$ Hz, 1H), 6.77 (s, 1H), 6.69 (d, $J = 8.0$ Hz, 1H), 4.02 (t, $J = 6.4$ Hz, 2H), 1.78–1.68 (m, 2H), 1.49–1.40 (m, 2H), 1.37–1.27 (m, 4H), 0.89 (t, $J = 7.0$ Hz, 3H). ^{13}C NMR (101 MHz, DMSO-d_6) δ 163.24, 159.07, 141.01, 136.84, 134.99, 129.49, 128.32, 127.42, 127.07, 126.95, 125.49, 125.01, 124.92, 124.44, 121.41, 118.62, 118.22, 114.88, 113.94, 113.74, 108.66, 67.58, 31.00, 28.62, 25.19, 22.06, 13.88. IR (KBr) ν : 3054, 2933, 2863, 2216, 1611, 1509, 1459, 1391, 1353, 1286, 1247, 1176, 1032, 936, 839, 796, 752, 723 cm^{-1} . HRMS (MALDI-TOF): m/z [M+H]⁺ calcd for $\text{C}_{34}\text{H}_{29}\text{N}_2\text{O}_4\text{S}$, 561.1848; found, 561.1848.

2.3.9. (*E*)-2-Cyano-3-(5''-(1-(4-(hexyloxy)phenyl)pyrrolo[3,2,1-*kl*]-phenothiazin-4-yl)-3,3''-diethyl-[2,2':5',2''-terthiophene]-5-yl)acrylic acid (**JY42**)

JY42 was synthesized by the same procedure described for **JY40**, and the crude product was purified by column chromatography on silica gel using $\text{CH}_2\text{Cl}_2/\text{CH}_3\text{OH}$ (12:1) as the eluent to afford **JY42** as a deep red solid (95 mg, yield: 87%). ^1H NMR (400 MHz, DMSO- d_6) δ 8.28 (s, 1H), 7.76 (s, 1H), 7.44 (d, $J = 7.7$ Hz, 3H), 7.33 (d, $J = 4.0$ Hz, 2H), 7.25 (d, $J = 6.9$ Hz, 1H), 7.20–7.15 (m, 2H), 6.98 (m, 3H), 6.91 (t, $J = 7.8$ Hz, 1H), 6.66 (d, $J = 8.2$ Hz, 1H), 6.63 (s, 1H), 3.99 (t, $J = 6.4$ Hz, 2H), 2.75 (dd, $J = 16.2, 8.7$ Hz, 4H), 1.79–1.71 (m, 2H), 1.68–1.55 (m, 4H), 1.48–1.40 (m, 2H), 1.38–1.20 (m, 24H), 0.89 (t, $J = 6.9$ Hz, 3H), 0.82 (m, 6H). ^{13}C NMR (101 MHz, THF- d_8) δ 160.37, 141.84, 140.50, 138.97, 137.79, 136.74, 134.87, 134.53, 131.13, 130.20, 129.30, 128.65, 128.47, 127.50, 126.51, 126.24, 125.08, 123.23, 119.74, 119.27, 115.35, 115.29, 114.93, 109.27, 68.48, 32.71, 32.40, 31.21, 30.93, 30.48, 30.32, 30.24, 30.11, 30.03, 26.53, 23.39, 23.34, 14.30, 14.20. IR (KBr) ν : 3062, 2926, 2856, 2215, 1673, 1608, 1559, 1502, 1464, 1399, 1260, 1213, 1172, 1023, 936, 833, 789, 750 cm^{-1} . HRMS (MALDI-TOF): m/z [M+H] $^+$ calcd for $\text{C}_{58}\text{H}_{65}\text{N}_2\text{O}_3\text{S}_4$, 965.3878; found, 965.3879.

3. Results and discussion

3.1. Synthesis and characterization

As shown in **Scheme 1**, *para*-bromoaniline (**1**) was first treated with molecular I_2 in the presence of Ag_2SO_4 to give 4-bromo-2,6-diiodoaniline (**2**). Selective palladium catalyzed Sonogashira coupling was further achieved by controlling the molar ratio of reactant **2** and 1-ethynyl-4-(hexyloxy)benzene to afford mono-coupling product **3**. A Cu(I)-catalyzed tandem C–S coupling/double cyclization reaction was adopted to construct the tetracyclic fused key intermediate **4** [39]. With the pyrrolo[3,2,1-*kl*]-phenothiazine (**4**) in hand, a conventional Suzuki coupling with appropriate aldehyde substituted arylboronic acids was performed to yield precursors **6** and **7**. As for precursor **8**, the intermediate **4** was

first transformed into the corresponding boronic acid form, and subsequent Suzuki coupling reaction was carried out with bromo-substituted terthiophene [40]. Finally, the Knoevenagel condensations of compounds **6–8** with cyanoacetic acid were easily realized in the presence of ammonium acetate and acetic acid to produce the target dyes **JY40–42** [41].

3.2. Optical and electrochemical properties

The UV/Vis absorption spectra of the new dyes in CH_2Cl_2 solutions were measured and shown in **Fig. 2**, and the relevant data are summarized in **Table 1**. All dyes exhibit two distinct absorption bands in CH_2Cl_2 solutions, the high-energy bands ($\lambda < 370$ nm) correspond to the localized aromatic $\pi-\pi^*$ electronic transitions of the chromophores, and the other bands in the low-energy region ($\lambda > 370$ nm) can be ascribed to the intramolecular charge transfer (ICT) transitions from the donor to the acceptor of the chromophores [42,43]. The ICT absorption maximums (λ_{\max}) for dyes **JY40**, **JY41** and **JY42** are at 400, 418, and 461 nm, respectively. The

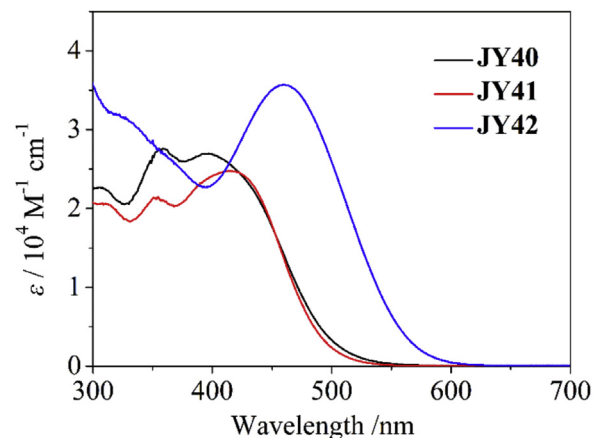
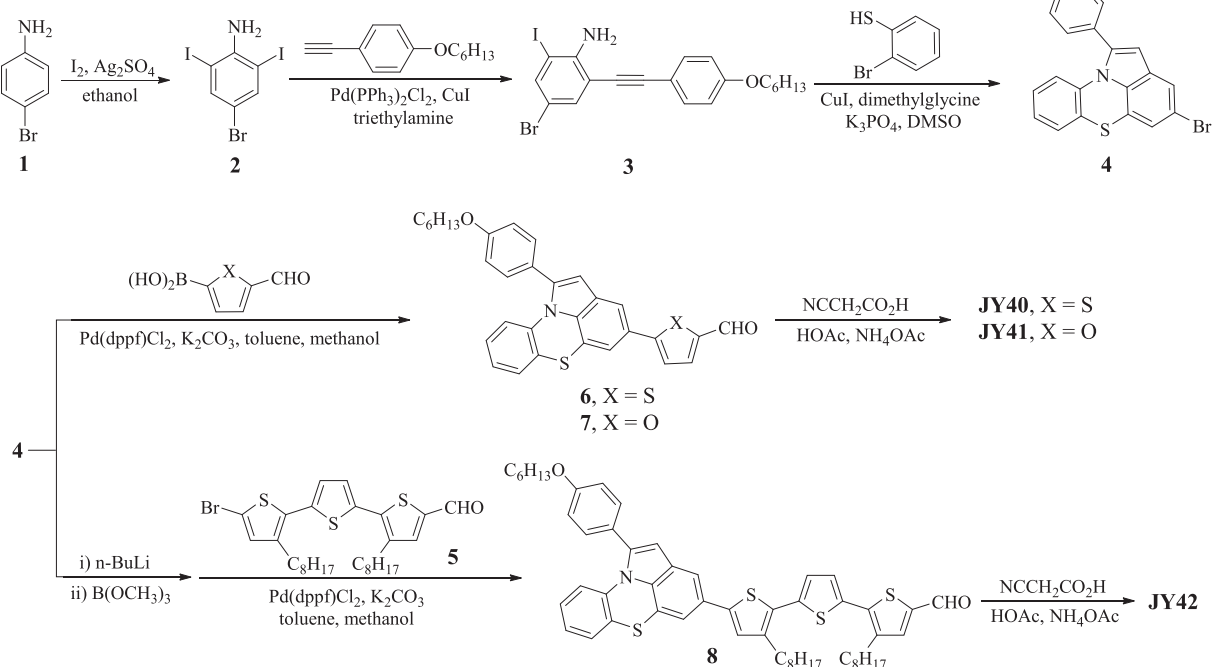


Fig. 2. UV-vis spectra of **JY40–42** in CH_2Cl_2 solutions.



Scheme 1. Synthetic routes for **JY40–42**.

Table 1Photophysical and electrochemical data of **JY40–42**.

Dye	$\lambda_{\text{max}}/\text{nm}^{\text{a}}$	$\varepsilon/10^4 \text{ M}^{-1} \text{ cm}^{-1}$	$E_{\text{ox}}/\text{V}^{\text{b}}$	$E_{0-0}/\text{eV}^{\text{c}}$	$E_{\text{ox}}^*/\text{V}^{\text{d}}$
JY40	400	2.69	1.13	2.17	-1.04
JY41	418	2.46	1.13	2.25	-1.12
JY42	461	3.57	1.06	2.01	-0.95

^a The absorption spectra were measured in CH_2Cl_2 solution ($3 \times 10^{-5} \text{ M}$) at room temperature.

^b First oxidation potentials (vs. NHE) were measured in benzonitrile with TBAPF₆ (0.1 M) as the supporting electrolyte (working electrode: glassy carbon; counter electrode: Pt wire; reference electrode: Ag/Ag⁺).

^c E_{0-0} values were estimated from the onset wavelength of the absorption spectra in CH_2Cl_2 solutions using $E_{0-0} = 1240/\lambda_{\text{onset}}$.

^d E_{ox}^* : The excited state oxidation potential, and $E_{\text{ox}}^* = E_{\text{ox}} - E_{0-0}$.

significantly red-shifted and enhanced ICT absorption band of dye **JY42** (461 nm, $35700 \text{ M}^{-1} \text{ cm}^{-1}$) compared to **JY40** (400 nm, $26900 \text{ M}^{-1} \text{ cm}^{-1}$) and **JY41** (418 nm, $24600 \text{ M}^{-1} \text{ cm}^{-1}$) is due to the better electron delocalization over the whole molecule with terthiophene as π -linker.

To evaluate the thermodynamic possibility of electron injection and dye regeneration, the oxidation potentials of dyes were measured in benzonitrile by using cyclic voltammetry (CV) with tetra-*n*-butylammonium hexafluorophosphate (TBAPF₆, 0.1 M) as the supporting electrolyte. Ferrocene/ferrocenium couple (Fc/Fc+, 0.63 V vs. NHE) was employed as an external reference [44,45], and the CV plots are displayed in Fig. 3. Corresponding to the first redox potential (E_{ox}), the highest occupied molecular orbital (HOMO) energy levels of **JY40–42** are 1.13, 1.13, and 1.06 V, respectively. The band gap energies (E_{0-0}) of **JY40–42** are 2.17, 2.25 and 2.01 eV, which are estimated from the onset wavelength of the absorption spectra of the dyes in CH_2Cl_2 solutions. The lowest unoccupied molecular orbital (LUMO) energy levels of **JY40–42** can be calculated by subtracting E_{0-0} from E_{ox} , and the values are -1.04, -1.12, and -0.95 V, respectively (Table 1). Based on the electrochemical data, the energy level diagrams are depicted in Fig. 4. All the LUMO levels of **JY40–42** are more negative than the conduction band (E_{cb}) of TiO_2 (-0.5 V vs. NHE). Meanwhile, all the HOMO levels of **JY40–42** are sufficiently more positive than the I^-/I_3^- redox potential (0.4 V vs. NHE). These results ensure favorable electron injection from excited dyes into the conduction band of TiO_2 upon photoexcitation and effective regeneration of the oxidized dye by the electrolyte.

3.3. Theoretical calculations

To gain a deep insight into the molecular structure and frontier

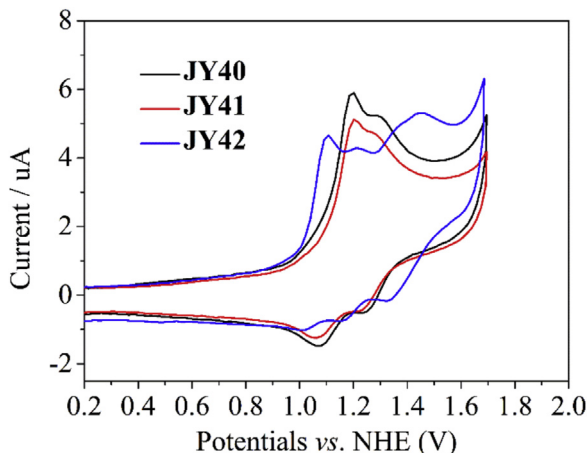


Fig. 3. Cyclic voltammograms of **JY40–42** recorded in benzonitrile solutions.

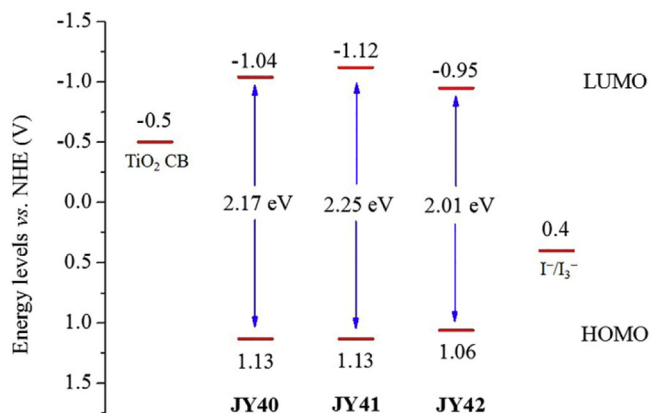


Fig. 4. Schematic energy-level diagrams of **JY40–42**.

orbital configurations, density functional theory (DFT) calculations were performed by using Gaussian 09 program package at the B3LYP/6-31 G(d) level [46,47]. The optimized geometries and electron distributions of the frontier molecular orbitals of **JY40–42** are shown in Fig. 5. In the ground state, the geometry of pyrrolo[3,2,1-kl]phenothiazine is not fully planar, and the angle between the indole unit and the phenyl ring is 152° from the nitrogen side. The nonplanar conformation of pyrrolo[3,2,1-kl]phenothiazine may impede dye aggregation and the formation of intermolecular excimer. The dihedral angles between the pyrrolo[3,2,1-kl]phenothiazine donor and the π -linker of **JY40–42** are estimated to be 27.1°, 0.9°, and 30.4°, respectively. For all dyes, the HOMO orbitals are delocalized from the pyrrolo[3,2,1-kl]phenothiazine donor to the cyanoacrylic acid acceptor, while the LUMO orbitals are mainly localized at the cyanoacrylic acid and its adjacent π -linkers. The HOMO and LUMO of the dyes displayed partial overlap between the donor group and the anchoring group, which would have a favorable effect on the charge separation within the dye and subsequent electron injection from the excited dye into the conduction band of TiO_2 upon photoexcitation.

3.4. Photovoltaic performance of DSSCs

The photovoltaic properties of the DSSCs sensitized by **JY40–42** under AM 1.5 G condition (100 mW cm^{-2}) were evaluated with an iodine electrolyte (0.3 M DMPII, 0.1 M LiI, 0.05 M I_2 and 0.5 M 4-*tert*-butylpyridine in acetonitrile). Pertinent parameters are listed in Table 2, and the photocurrent-voltage (*J*-*V*) curves are plotted in Fig. 6a. The cell based on **JY40** with a thiophene as the π -linker gave a PCE of 6.42%, with a short-circuit photocurrent density (J_{sc}) of 13.38 mA cm^{-2} , an open-circuit photovoltage (V_{oc}) of 736 mV and a fill factor (FF) of 0.65. When replacing the thiophene linker of **JY40** by furan, the resultant **JY41**-based cell showed decreased V_{oc} (705 mV) and J_{sc} (12.60 mA cm^{-2}), and hence showed a relatively lower PCE of 5.60%. This is probably due to its stronger aggregation on the TiO_2 surface resulted from the relatively smaller dihedral angle between the pyrrolo[3,2,1-kl]phenothiazine donor and the furan linker. The increased V_{oc} and J_{sc} of **JY41** with co-adsorbent chenodeoxycholic acid (CDCA) compared to that without CDCA in the photovoltaic experiments (Supporting Information, Fig. S1 and Table S1) also confirms the more serious aggregating tendency of dye **JY41**. Notably, **JY42** with terthiophene π -spacer gave a significantly improved J_{sc} (17.76 mA cm^{-2}) due to its much broadened and enhanced ICT absorption arised from its greatly extended conjugated structure. Although undesirable dye aggregation and charge recombination aroused simultaneously by the expanded molecular

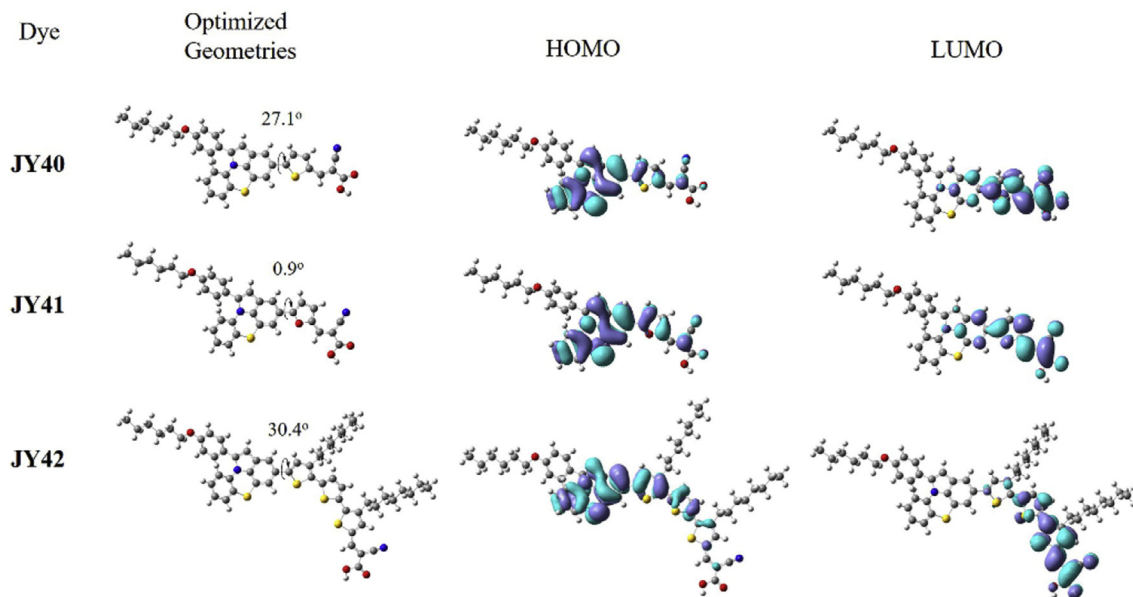


Fig. 5. The geometries and frontier orbitals of **JY40–42** optimized by DFT calculations.

Table 2
Photovoltaic performance of **JY40–42** with **N719** as a reference.^a

Dye	DL/nmol cm ⁻²	V _{oc} /mV	J _{sc} /mA cm ⁻²	FF	PCE/%
JY40	158	736	13.38	0.65	6.42
JY41	175	705	12.60	0.63	5.60
JY42	136	726	17.76	0.58	7.54
N719	—	762	17.40	0.60	7.95

^a Active area of the cells was 0.196 cm²; DL was the amount of dye loading; The **N719**-sensitized cell was immersed in the commercial **N719** dye solution (0.3 mM in ethanol) for 12 h.

structure led to a relative low V_{oc} (726 mV) compared to **JY40** (736 mV), **JY42** finally achieved the highest PCE of 7.54%. This reaches about 95% of the ruthenium dye **N719**-based standard cell under the same conditions. As mentioned above, all these dyes showed a high V_{oc} over 700 mV and moderate J_{sc} over 12.6 mA cm⁻², which are comparable to those of the phenothiazine/phenoxyazine-based dyes with similar structures [48,49], demonstrating pyrrolo[3,2,1-kl]phenothiazine is a promising electron donor to be used to construct highly efficient solar cells.

To analyze the effect of π-linker on the photocurrent features, the incident photon-to-current conversion efficiency (IPCE) spectra of **JY40–42** were performed. As shown in Fig. 6b, the onsets of **JY40** and **JY41** were observed at 650 and 620 nm, respectively. In comparison to that of **JY41**, the red-shift of the IPCE onset for **JY40** can be attributed to the more electron-rich feature of thiophene relative to furan. Furthermore, the conjugation-extended terthiophene linker causes a much better electron delocalization over the whole molecule, thus the onset of **JY42** was significantly red-shifted to 750 nm. Notably, over 60% IPCE value can be observed for **JY42**-based cell in a broad region ranged from 380 to 620 nm, accompanying with a maximum IPCE value of 85% at 450 nm. The broader IPCE response range and higher IPCE values of **JY42** explains its highest measured J_{sc} value.

3.5. Electrochemical impedance spectroscopy

To further understand the photovoltaic behavior of the DSSCs, electrochemical impedance spectroscopy (EIS) was carried out in

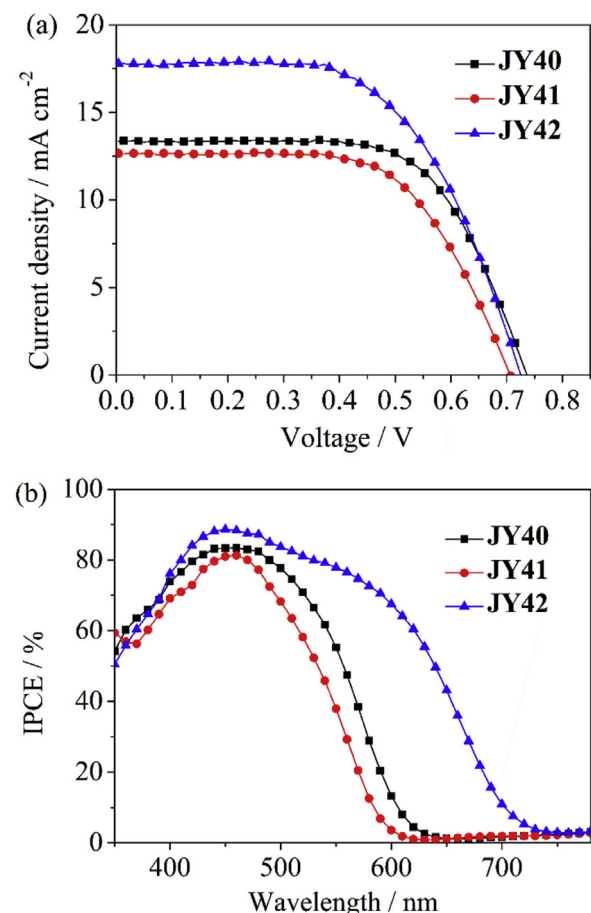


Fig. 6. (a) The photocurrent density-voltage (J-V) curves and (b) the IPCE spectra of **JY40–42**.

the dark under a forward bias of -0.70 V with frequency range of 0.1–100 kHz. For the Nyquist plots (Fig. 7a), the larger semicircle is related to the charge recombination resistance (R_{rec}) at the TiO₂/

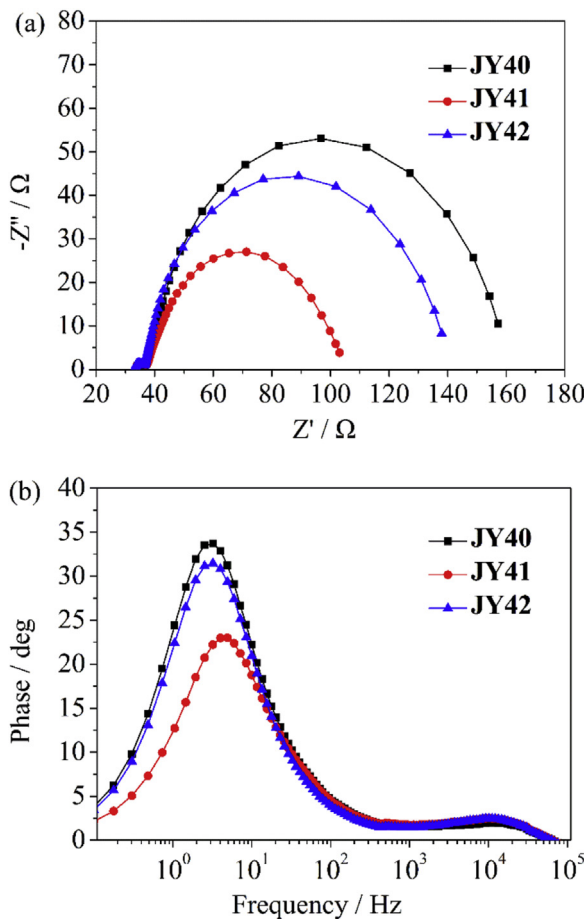


Fig. 7. (a) Nyquist plots and (b) Bode phase plots for DSSCs based on **JY40-42** measured in the dark under -0.70 V bias.

dye/electrolyte interface. The larger the radius of the semicircle is, the smaller the rate for electron recombination at the interface is. A smaller R_{rec} means faster charge recombination rate, indicating a larger dark current and lower V_{oc} [50,51]. The fitted R_{rec} increased in the order of **JY41** (57.8Ω) < **JY42** (92.8Ω) < **JY40** (109.9Ω), which is consistent with the order of the V_{oc} values of **JY41** (705 mV) < **JY42** (726 mV) < **JY40** (736 mV).

In the Bode phase plots of the devices (Fig. 7b), the characteristic frequency peak (f) in the intermediate-frequency regime is correlated with the electron lifetime in the TiO_2 film. The electron lifetime (τ_e) can be calculated using $\tau_e = 1/(2\pi f)$ [52,53], and the values of τ_e increased in the order of **JY41** (35.2 ms) < **JY42** (49.5 ms) < **JY40** (54.2 ms). In general, a longer electron lifetime means more effective suppression of back reaction of injected electrons with I_3^- ions in the electrolyte, which results in a higher V_{oc} [53,54]. So the order of the V_{oc} values of **JY40-42** can be further explained.

4. Conclusions

In summary, three novel metal-free organic dyes containing pyrrolo[3,2,1-kl]-phenothiazine moiety as the electron donor have been designed and synthesized. Simple spacers such as thiophene (**JY40**), furan (**JY41**), and terthiophene (**JY42**) were employed as conjugated bridge to construct the D- π -A sensitizer structure, and show great influence on the photophysical, electrochemical and photovoltaic properties of the resulting dyes. All the synthesized dyes showed good ability for light-energy conversion, and cell

based on **JY42** exhibited an attractive PCE up to 7.54% , with a J_{sc} of 17.76 mA cm^{-2} , a V_{oc} of 726 mV, and a FF of 0.58 under standard AM 1.5 G irradiation in conjunction with an iodine electrolyte. These results suggest that pyrrolo[3,2,1-kl]phenothiazine is a promising electron donor for high-performance DSSCs.

Acknowledgements

We are grateful to the 973 Program (2011CB932502), the National Natural Science Foundation of China (Nos: 21572108 and 21272123) and Tianjin Natural Science Foundation (16JCYBJC16700) for their financial support.

Appendix A. Supplementary data

Supplementary data related to this article can be found at <http://dx.doi.org/10.1016/j.dyepig.2016.12.025>.

References

- [1] O'Regan B, Grätzel M. A low-cost, high-efficiency solar cell based on dye-sensitized colloidal TiO_2 films. *Nature* 1991;353:737–40.
- [2] Grätzel M. Recent advances in sensitized mesoscopic solar cells. *Acc Chem Res* 2009;42:1788–98.
- [3] Hagfeldt A, Boschloo G, Sun L, Kloo L, Pettersson H. Dye-sensitized solar cells. *Chem Rev* 2010;110:6595–663.
- [4] Nazeeruddin MK, Kay A, Rodicio I, Humphry-Baker R, Mueller E, Liska P, et al. Conversion of light to electricity by *cis*-X- $\text{bis}(2,2'\text{-bipyridyl}-4,4'\text{-dicarboxylate})$ ruthenium(II) charge-transfer sensitizers ($X = \text{Cl}^-$, Br^- , I^- , CN^- , and SCN^-) on nanocrystalline titanium dioxide electrodes. *J Am Chem Soc* 1993;115:6382–90.
- [5] Nazeeruddin MK, Péchy P, Renouard T, Zakeeruddin SM, Humphry-Baker R, Comte P, et al. Engineering of efficient panchromatic sensitizers for nanocrystalline TiO_2 -based solar cells. *J Am Chem Soc* 2001;123:1613–24.
- [6] Nazeeruddin MK, De Angelis F, Fantacci S, Selloni A, Viscardi G, Liska P, et al. Combined experimental and DFT-TDDFT computational study of photoelectrochemical cell ruthenium sensitizers. *J Am Chem Soc* 2005;127:16835–47.
- [7] Li LL, Diau EW-G. Porphyrin-sensitized solar cells. *Chem Soc Rev* 2013;42:291–304.
- [8] Urbani M, Grätzel M, Nazeeruddin MK, Torres T. Meso-substituted porphyrins for dye-sensitized solar cells. *Chem Rev* 2014;114:12330–96.
- [9] Higashino T, Imahori H. Porphyrins as excellent dyes for dye-sensitized solar cells: recent developments and insights. *Dalton Trans* 2015;44:448–63.
- [10] Ahmad S, Guillén E, Kavan L, Grätzel M, Nazeeruddin MK. Metal free sensitizer and catalyst for dye sensitized solar cells. *Energy Environ Sci* 2013;6:3439–66.
- [11] Liang M, Chen J. Arylamine organic dyes for dye-sensitized solar cells. *Chem Soc Rev* 2013;42:3453–88.
- [12] Wu Y, Zhu W. Organic sensitizers from D- π -A to D-A- π -A: effect of the internal electron-withdrawing units on molecular absorption, energy levels and photovoltaic performances. *Chem Soc Rev* 2013;42:2039–58.
- [13] Mathew S, Yella A, Gao P, Humphry-Baker R, Curchod BF, Ashari-Astani N, et al. Dye-sensitized solar cells with 13% efficiency achieved through the molecular engineering of porphyrin sensitizers. *Nat Chem* 2014;6:242–7.
- [14] Kakiage K, Aoyama Y, Yano T, Otsuka T, Kyomen T, Unno M, et al. An achievement of over 12 percent efficiency in an organic dye-sensitized solar cell. *Chem Commun* 2014;50:6379–81.
- [15] Kakiage K, Aoyama Y, Yano T, Oya K, Fujisawa J-i, Hanaya M. Highly-efficient dye-sensitized solar cells with collaborative sensitization by silyl-anchor and carboxy-anchor dyes. *Chem Commun* 2015;51:15894–7.
- [16] Yao Z, Zhang M, Li R, Yang L, Qiao Y, Wang P. A metal-free *N*-annulated thienocyclopentaperylene dye: power conversion efficiency of 12% for dye-sensitized solar cells. *Angew Chem Int Ed* 2015;54:5994–8.
- [17] Yao Z, Zhang M, Wu H, Yang L, Li R, Wang P. Donor/acceptor indenoperylene dye for highly efficient organic dye-sensitized solar cells. *J Am Chem Soc* 2015;137:3799–802.
- [18] Kitamura T, Ikeda M, Shigaki K, Inoue T, Anderson NA, Ai X, et al. Phenyl-conjugated oligoene sensitizers for TiO_2 solar cells. *Chem Mater* 2004;16:1806–12.
- [19] Kim S, Lee JK, Kang SO, Ko J, Yum JH, Fantacci S, et al. Molecular engineering of organic sensitizers for solar cell applications. *J Am Chem Soc* 2006;128:16701–7.
- [20] Zeng W, Cao Y, Bai Y, Wang Y, Shi Y, Zhang M, et al. Efficient dye-sensitized solar cells with an organic photosensitizer featuring orderly conjugated ethylenedioxothiophene and dithienosilole blocks. *Chem Mater* 2010;22:1915–25.
- [21] Zhou N, Prabakaran K, Lee B, Chang SH, Harutyunyan B, Guo P, et al. Metal-free tetraphienoacene sensitizers for high-performance dye-sensitized solar

- cells. *J Am Chem Soc* 2015;137:4414–23.
- [22] Koumura N, Wang Z-S, Mori S, Miyashita M, Suzuki E, Hara K. Alkyl-functionalized organic dyes for efficient molecular photovoltaics. *J Am Chem Soc* 2006;128:14256–7.
- [23] Huang J-F, Liu J-M, Tan L-L, Chen Y-F, Shen Y, Xiao L-M, et al. Novel carbazole based sensitizers for efficient dye-sensitized solar cells: role of the hexyl chain. *Dyes Pigm* 2015;114:18–23.
- [24] Kakiage K, Aoyama Y, Yano T, Oya K, Kyomen T, Hanaya M. Fabrication of a high-performance dye-sensitized solar cell with 12.8% conversion efficiency using organic silyl-anchor dyes. *Chem Commun* 2015;51:6315–7.
- [25] Tian H, Yang X, Chen R, Pan Y, Li L, Hagfeldt A, et al. Phenothiazine derivatives for efficient organic dye-sensitized solar cells. *Chem Commun* 2007:3741–3.
- [26] Hua Y, Chang S, Huang D, Zhou X, Zhu X, Zhao J, et al. Significant improvement of dye-sensitized solar cell performance using simple phenothiazine-based dyes. *Chem Mater* 2013;25:2146–53.
- [27] Huang Z-S, Meier H, Cao D. Phenothiazine-based dyes for efficient dye-sensitized solar cells. *J Mater Chem C* 2016;4:2404–26.
- [28] Tian H, Yang X, Cong J, Chen R, Liu J, Hao Y, et al. Tuning of phenoxazine chromophores for efficient organic dye-sensitized solar cells. *Chem Commun* 2009;6288–90.
- [29] Karlsson KM, Jiang X, Eriksson SK, Gabrielsson E, Rensmo H, Hagfeldt A, et al. Phenoxazine dyes for dye-sensitized solar cells: relationship between molecular structure and electron lifetime. *Chem Eur J* 2011;17:6415–24.
- [30] Yao Z, Wu H, Ren Y, Guo Y, Wang P. A structurally simple perylene dye with ethynylbenzothiadiazole-benzoic acid as the electron acceptor achieves an over 10% power conversion efficiency. *Energy Environ Sci* 2015;8:1438–42.
- [31] Qian X, Zhu Y-Z, Song J, Gao X-P, Zheng J-Y. New donor- π -acceptor type triazatruxene derivatives for highly efficient dye-sensitized solar cells. *Org Lett* 2013;15:6034–7.
- [32] Qian X, Gao H-H, Zhu Y-Z, Pan B, Zheng J-Y. Tetraindole-based saddle-shaped organic dyes for efficient dye-sensitized solar cells. *Dyes Pigm* 2015;121:152–8.
- [33] Zhang X-H, Cui Y, Katoh R, Koumura N, Hara K. Organic dyes containing thieno [3,2-b]indole donor for efficient dye-sensitized solar cells. *J Phys Chem* 2010;114:18283–90.
- [34] Cai S, Tian G, Li X, Su J, Tian H. Efficient and stable DSSC sensitizers based on substituted dihydroindolo[2,3-b]carbazole donors with high molar extinction coefficients. *J Mater Chem A* 2013;1:11295–305.
- [35] Zhao J, Oniwa K, Islam A, Qin C, Asao N, Han L, et al. Thieno[2,3,a]carbazole donor-based organic dyes for high efficiency dye-sensitized solar cells. *Org Chem Front* 2015;2:253–8.
- [36] Qian X, Gao H-H, Zhu Y-Z, Lu L, Zheng J-Y. 6H-Indolo[2,3-b]quinoxaline-based organic dyes containing different electron-rich conjugated linkers for highly efficient dye-sensitized solar cells. *J Power Sources* 2015;280:573–80.
- [37] Qian X, Zhu Y-Z, Chang WY, Song J, Pan B, Lu L, et al. Benzo[a]carbazole-based donor- π -acceptor type organic dyes for highly efficient dye-sensitized solar cells. *ACS Appl Mater Interfaces* 2015;7:9015–22.
- [38] Hollins RA, Pinto AC. A synthesis of pyrrolo[3,2,1-kl]phenothiazine and derivatives. *J Heterocycl Chem* 1978;15:711–3.
- [39] Tang J, Xu B, Mao X, Yang H, Wang X, Lv X. One-pot synthesis of pyrrolo[3,2,1-kl]phenothiazines through copper-catalyzed tandem coupling/double cyclization reaction. *J Org Chem* 2015;80:11108–14.
- [40] Xie Y, Wu W, Zhu H, Liu J, Zhang W, Tian H, et al. Unprecedentedly targeted customization of molecular energy levels with auxiliary-groups in organic solar cell sensitizers. *Chem Sci* 2016;7:544–9.
- [41] Wang D, Ying W, Zhang X, Hu Y, Wu W, Hua J. Near-infrared absorbing isoindigo sensitizers: synthesis and performance for dye-sensitized solar cells. *Dyes Pigm* 2015;112:327–34.
- [42] Wang Z, Wang H, Liang M, Tan Y, Cheng F, Sun Z, et al. Judicious design of indoline chromophores for high-efficiency iodine-free dye-sensitized solar cells. *ACS Appl Mater Interfaces* 2014;6:5768–78.
- [43] Wu Z, Li X, Li J, Agren H, Hua J, Tian H. Effect of bridging group configuration on photophysical and photovoltaic performance in dye-sensitized solar cells. *J Mater Chem A* 2015;3:14325–33.
- [44] Kim SH, Choi J, Sakong C, Namgoong JW, Lee W, Kim DH, et al. The effect of the number, position, and shape of methoxy groups in triphenylamine donors on the performance of dye-sensitized solar cells. *Dyes Pigm* 2015;113:390–401.
- [45] Qian X, Lu L, Zhu Y-Z, Gao H-H, Zheng J-Y. Triazatruxene-based organic dyes containing a rhodanine-3-acetic acid acceptor for dye-sensitized solar cells. *Dyes Pigm* 2015;113:737–42.
- [46] Li X, Hu Y, Sanchez-Molina I, Zhou Y, Yu F, Haque SA, et al. Insight into quinoxaline containing D- π -A dyes for dye-sensitized solar cells with cobalt and iodine based electrolytes: the effect of π -bridge on the HOMO energy level and photovoltaic performance. *J Mater Chem A* 2015;3:21733–43.
- [47] Karthik D, Kumar V, Justin Thomas KR, Li C-T, Ho K-C. Synthesis and characterization of thieno[3,4-d]imidazole-based organic sensitizers for photoelectrochemical cells. *Dyes Pigm* 2016;129:60–70.
- [48] Kim SH, Kim HW, Sakong C, Namgoong J, Park SW, Ko MJ, et al. Effect of five-membered heteroaromatic linkers to the performance of phenothiazine-based dye-sensitized solar cells. *Org Lett* 2011;13:5784–7.
- [49] Lee W, Choi J, Namgoong JW, Kim SH, Sun KC, Jeong SH, et al. The effect of five-membered heterocyclic bridges and ethoxyphenyl substitution on the performance of phenoxazine-based dye-sensitized solar cells. *Dyes Pigm* 2014;104:185–93.
- [50] Wang Q, Moser J-E, Grätzel M. Electrochemical impedance spectroscopic analysis of dye-sensitized solar cells. *J Phys Chem B* 2005;109:14945–53.
- [51] Adachi M, Sakamoto M, Jiu J, Ogata Y, Isoda S. Determination of parameters of electron transport in dye-sensitized solar cells using electrochemical impedance spectroscopy. *J Phys Chem B* 2006;110:13872–80.
- [52] Chang S, Wang H, Lin Lee LT, Zheng S, Li Q, Wong KY, et al. Panchromatic light harvesting by N719 with a porphyrin molecule for high-performance dye-sensitized solar cells. *J Mater Chem C* 2014;2:3521–6.
- [53] Venkateswararao A, Thomas KRJ, Lee C-P, Li C-T, Ho K-C. Organic dyes containing carbazole as donor and π -linker: optical, electrochemical, and photovoltaic properties. *ACS Appl Mater Interfaces* 2014;6:2528–39.
- [54] Iqbal Z, Wu W-Q, Huang Z-S, Wang L, Kuang D-B, Meier H, et al. Trilateral π -conjugation extensions of phenothiazine-based dyes enhance the photovoltaic performance of the dye-sensitized solar cells. *Dyes Pigm* 2016;124:63–71.